ISSN 0915-633X

NATIONAL INSTITUTE FOR FUSION SCIENCE

Extraction of Negative Pionlike Particles from a H_2 or D_2 Gas Discharge Plasma in Magnetic Field

J. Uramoto

(Received - Sep. 4, 1995)

NIFS-377 Sep. 1995

RESEARCH REPORT
NIFS Series

NAGOYA, JAPAN

Extraction of negative pionlike particles from a H_2 or D_2 gas discharge plasma in magnetic field

Jōshin URAMOTO

National Institute of Fusion Science,

Nagoya 464-01, Japan

Abstract

Electron density in outside region of H_2 or D_2 gas discharge plasma along magnetic field, is abruptly reduced as H^- or D^- ions are produced. From the region, negative pionlike particles are extracted together with H^- or D^- ions. Then, a positive bias voltage is necessary for the beam collector of magnetic mass analyzer.

Keywords: negative pionlike particle π^-, H_2 gas discharge, H^- ion

In ordinary plasmas, strong electrical interactions between electron bunches and positive ion bunches are not generated through charge neutralization between electron space charge and positive ion space charge. But, two exceptional cases are considerable: (1) In the outside region of H_2 or D_2 gas discharge plasma along magnetic field, the electron density is abruptly reduced in comparison to the positive ion density by the volume produced H^- or D^- ions[1,2,3] which absorb the low energy electrons. Therefore, some strong interactions between the electron bunches and the positive ion bunches are expected to produce some elementary particles. (2) By decelerating an electron beam and a positive ion beam magnetically or electrically, an electron bunch and a positive ion bunch are produced while their two bunches are mixed.

For the above case of (2), we have reported[4,5] already as productions of pionlike particle π^- and muonlike particle μ^-. However, the experimental facts may be difficult to understand as the electron bunch (magnetical) and the positive ion bunch (electrical) are produced and mixed around the entrance of magnetic mass analyzer while the mass analysis is done.

In this paper, the above case of (1) will be investigated. Then, some negative charged particles are extracted from the H_2 or D_2 gas discharge plasma by the typical three extraction electrodes, where the ordinary magnetic deflection-type mass analysis is tried. Only, it is different from the ordinary analysis that a positive bias voltage is given for the beam collector of the analyzer.

A schematic diagram of the experimental apparatus is shown in Fig. 1. The apparatus is constructed from a H_2 or D_2 gas discharge plasma in magnetic fields, three extraction electrodes (with an aperture of 3 mm in diameter) to extract some negatively charged particles and a magnetic mass analyzer (90° deflection-type).

An electron acceleration-type sheet plasma[6] is produced to generate H^- or D^- ions effectively and in wide area. That is, the discharge (cylindrical) plasma flow of about 1 cm in diameter is transformed into a sheet plasma flow of about 3 mm in thickness and about 20 cm in width, while the electron components in the initial discharge plasma are accelerated near 80 eV. The sheet plasma flow passes through the electron acceleration anode (12 in Fig. 1) and enters the main chamber (50 cm long). The electron components in the sheet plasma are reflected by the end plate which is electrically floated. A uniform magnetic field of about 50 gauss is applied along the sheet plasma flow in the main chamber where the H_2 or D_2 gas pressure is about 1.5×10^{-3} Torr.

The electron acceleration anode current I_A is 20A and about 60% of I_A enters the main chamber. A distance between the sheet plasma center and the first extraction electrode (L) is 7.5 cm. The plasma density in the center of the sheet plasma is about 10^{11}/cc and the electron temperature is about 20 eV. The positive ion density in front of the first extraction electrode is estimated to be about 7.5×10^9/cc from a positive ion saturation current as H_3^+, while the electron density from the Langmuir probe characteristic is about 8.2×10^8/cc and the electron temperature is about 3.0 eV. That is, the electron density in front of the first extraction electrode is reduced near 1/10 of the positive ion density. It is estimated from the beam collector current of the magnetic analyzer that the extracted H^- ion current density is comparable to the extracted H_3^+ ion current density.

The negatively charged particles extracted from the H_2 or D_2 gas discharge plasma, are injected into the ordinary magnetic mass analyzer (MA) through the slit (3 mm × 1 cm) while each mass of the negatively charged particle is estimated by the following relations: From the analyzing magnetic field B_M where the negative current to the beam collector BC shows a peak, the curvature radius r of the mass analyzer and the extraction (acceleration) voltage V_E, we can estimate the mass m of the negatively charged particle by,

$$m = \frac{Ze\,(B_M r)^2}{2V_E}$$

$$= \frac{8.8 \times 10^{-2}\, Z\,(B_M r)^2\, m_e}{V_E}, \quad \text{..... (1)}$$

where e is the electron charge, B_M is in gauss unit, r is in cm unit, V_E is in volt unit and m_e is the electron mass and Z is the charge number. For the curvature radius $r = 4.3$ cm of this mass analyzer, the Eq. (1) is rewritten by

$$m = \frac{1.63\, Z\, B_M^2}{V_E}\, m_e. \quad \text{..... (2)}$$

In the extraction of negatively charged particles, the first extraction electrode (L) is electrically floated, whose potential V_L is about −15V with respect to the electron acceleration anode (12 in Fig. 1). A potential V_M of the second extraction electrode (M) is kept at 100V. The potential V_E of the final extraction electrode (E) is varied from 400V to 1200V.

An result of the mass analysis for extraction of negatively charged particles from the H_2 gas discharge plasma, is shown in Fig. 2. Dependences of the negative current I^- to the beam collector on the analyzing magnetic field B_M are shown under $V_E = 400V$, 800V and 1200V. In these analyses, the bias voltage V_{BC} of the beam collector is kept at +25V with respect to the mass analyzer.

For $V_E = 400V$ [(1) of Fig. 2], the first peak of negative current I^- to the beam collector is seen at $B_M \approx 276$ gauss while the second peak appears at $B_M \approx 665$ gauss. From Eq.(2), we obtain $m_1 \approx 284$ me for the first peak and $m_2 \approx 1804$ me, assuming that $Z = 1$. Similarly, for $V_E = 800V$ [(2) for Fig. 2], the first peak of I^- is seen at $B_M \approx 384$ gauss while the second peak appears at $B_M \approx 957$ gauss. From Eq. (2), we obtain $m_1 \approx 300$ me for the first peak and $m_2 \approx 1868$ me. Finally, for $V_E = 1200V$ [(3) of Fig. 2], the first peak of I^- is seen at $B_M \approx 500$ gauss while the second peak appears at $B_M \approx 1167$ gauss. From Eq. (2), we obtain $m_1 \approx 315$ me for the first peak and $m_2 \approx 1850$ me.

Another result of the mass analysis for extraction of negatively charged particles from the D_2 gas discharge plasma, is shown in Fig. 3. Dependences of the negative current I^- to the beam collector, on the analyzing magnetic field B_M are shown under $V_E = 400V$ and 800V. For $V_E = 400V$ [(1) of Fig. 3], the first peak of I^- is seen at $B_M \approx 276$ gauss (which agrees with the case of H_2 gas), while the second peak appears at $B_M \approx 931$ gauss. From Eq. (2), we obtain $m_1 \approx 284$ me for the first peak and $m_2 \approx 3532$ me. For $V_E = 800V$ [(2) of Fig. 3], the first peak of I^- is seen at $B_M \approx 384$ gauss (which agrees with the case of H_2 gas), while the second peak appears at $B_M \approx 1392$ gauss. From Eq. (2), we obtain $m_1 \approx 300$ me for the first peak and $m_2 \approx 3950$ me.

From the above results for H_2 or D_2 gas plasma, we can estimate that the first particle mass (m_1) is near the typical negative pion mass (= 273 me) within 15% and the second particle mass (m_2) is near H^- ion mass (= 1840 me) or D^- ion mass (= 3680 me) within 7%.

Dependences of the first negative current peak and the second negative peak current on the beam collector bias voltage V_{BC} of the mass analyzer, are shown in Fig. 4. The first peak current (corresponding to the negative pionlike particle π^-) is varied (20 ~ 30) times by the bias voltages from 0V to 50V while the second peak current (corresponding to the H^- ion) is kept only within 1.3 times. Thus, a difference of physical character between the first peak particle and the second peak particle is clarified.

In the experiment of Fig. 5, a Cu plate of 0.5 mm in thickness is put in front of the beam collector of the mass analyzer. Then, the second current peak corresponding to H^- ion disappears while only the first current peak appears without decay. This experimental fact shows that the pionlike particle π^- penetrates the Cu plate without energy loss. It has been reported[7] already that the pionlike π^- or muonlike particle μ^- penetrates a metal plate if the positive ions exist behind the metal plate. In this experiment, those positive ions may be produced by the gas ionization due to the pionlike particle π^- itself.

We consider that the pionlike particles π^- outside of the H_2 or D_2 gas discharge plasma are generated by reducing low energy electrons through production of H^- ions or D^- ions. To confirm this consideration, a He or Ar gas discharge (sheet) plasma was produced in the main chamber. Thus, each mass analysis by the extraction electrodes was tried. As each result, no current peaks of negative charged particles to the beam collector were observed. Then, each negative current to the final extraction electrode (I_E in Fig. 1) and the mass analyzer body (I_{MA} in Fig. 1), increased (10 ~ 20) times in comparison with the case of H_2 or D_2 gas discharge plasma (normalized by the positive ion current). This fact means that each electron density (for the He or Ar gas discharge plasma) in front of the first extraction electrode (L) increased (10 ~ 20) times in comparison with the case of H_2 or D_2 gas. That is, a normal charge neutralization in the plasma by the He or Ar gas discharge, is kept between electrons and positive ions. This fact is also confirmed by a Langmuir probe characteristic in front of the first extraction electrode.

In conclusion, the pionlike particles π^- generate in outside region of the H_2 or D_2 gas discharge plasma where a charge neutralization between electrons and positive ions is lost remarkably. To detect the pionlike particles in the mass analyzer, a positive bias voltage with respect to the mass analyzer, must be given for the beam collector. We consider that the positive bias voltage of the beam collector is necessary to attract the pionlike or muonlike particles penetrating the beam collector itself.

References

1) J.M. Wadehra: *Appl. Phys. Lett.* **35** (1979) 917.

2) M. Bacal and G.W. Hamilton: *Phys. Rev. Lett.* **42** (1979) 1538.

3) M. Allan and S.F. Wong: *Phys. Rev. Lett.* 41 (1978) 1971.

4) J. Uramoto: National Institute of Fusion Science, Nagoya, Japan-Research Report, NIFS-266 (1993).

5) J. Uramoto: NIFS-277 (1994).

6) J. Uramoto: Journal of the vacuum society of Japan, **37** (1994) 507 in Japanese.

7) J. Uramoto: NIFS-350 (1995).

Figure Captions

Fig. 1 Schematic diagram of experimental apparatus.

1: Cylindrical plasma in discharge anode. 2: Discharge cathode. 3: H_2 or D_2 gas flow. 4: Discharge power supply. 5: Electron acceleration power supply. 6: Vacuum pump. 7: Area where cylindrical plasma is transformed into sheet plasma. 8: Insulation tube. 9: A pair of permanent magnets. 10: Magnetic field coils. 11: slit of acceleration anode. 12: Electron acceleration anode. 13: Floated end electrode. I_A: Current to Electron acceleration anode. CP: Cylindrical plasma. SP: Sheet plasma. B_2: Magnetic field. L: First extraction electrode. M: Second extraction electrode. E: Final extraction electrode. V_M: Potential of second extraction electrode with respect to electron acceleration anode. V_E: Potential of final extraction electrode with respect to electron acceleration anode. I_E : Negative current to final extraction electrode. MA: Magnetic deflection (90°) mass analyzer. B_M: Magnetic field intensity of MA. BC: Beam collector of MA. V_{BC}: Positive potential of BC with respect to MA. I^-: Negative current to BC. I_{MA}: Total negative current to MA. H_0^-: Hydrogen negative ions outside of sheet plasma. H^-: Accelerated hydrogen negative ions. π_0^-: Negative pionlike particles outside of sheet plasma. π^-: Accelerated negative pionlike particles.

Fig. 2 Dependences (for H_2 gas) of negative current I^- to beam collector on magnetic field intensity B_M of MA.

π^-: First peak of I^- corresponding to negative pionlike particle. H^-: Second peak of I^- corresponding to hydrogen negative ion. (1): Dependence at final extraction electrode potential $V_E = 400V$. (2) Dependence at $V_E = 800V$. (3): Dependence at $V_E = 1200V$.

Fig. 3 Dependences (for D_2 gas) of negative current I^- on B_M.

π^-: First peak of I^-. D^-: Second peak of I^- corresponding to deuteron negative ion. (1) Dependence at final extraction electrode potential $V_E = 400V$. (2): Dependence at $V_E = 800V$.

Fig. 4 Dependences of negative current I^- on B_M under various beam collector potential V_{BC}.

π^-: First peak of I^-. H^-: Second peak of I^- corresponding to negative hydrogen ion. 0V, 15V, 25V and 50V: Beam collector (bias) potentials V_{BC} with respect to MA. $V_E = 800V$.

Fig. 5 Dependences of negative current I^- on B_M under a case setting a Cu plate in front of beam collector. $V_E = 800V$.

π^-: First peak of I^- corresponding to negative pionlike particle. (H^-): Position of second peak of I^-. Cu: Copper plate of 0.5 mm in thickness, which shields the surface of beam collector. (1): $V_{BC} = 25V$. (2): $V_{BC} = 50V$.

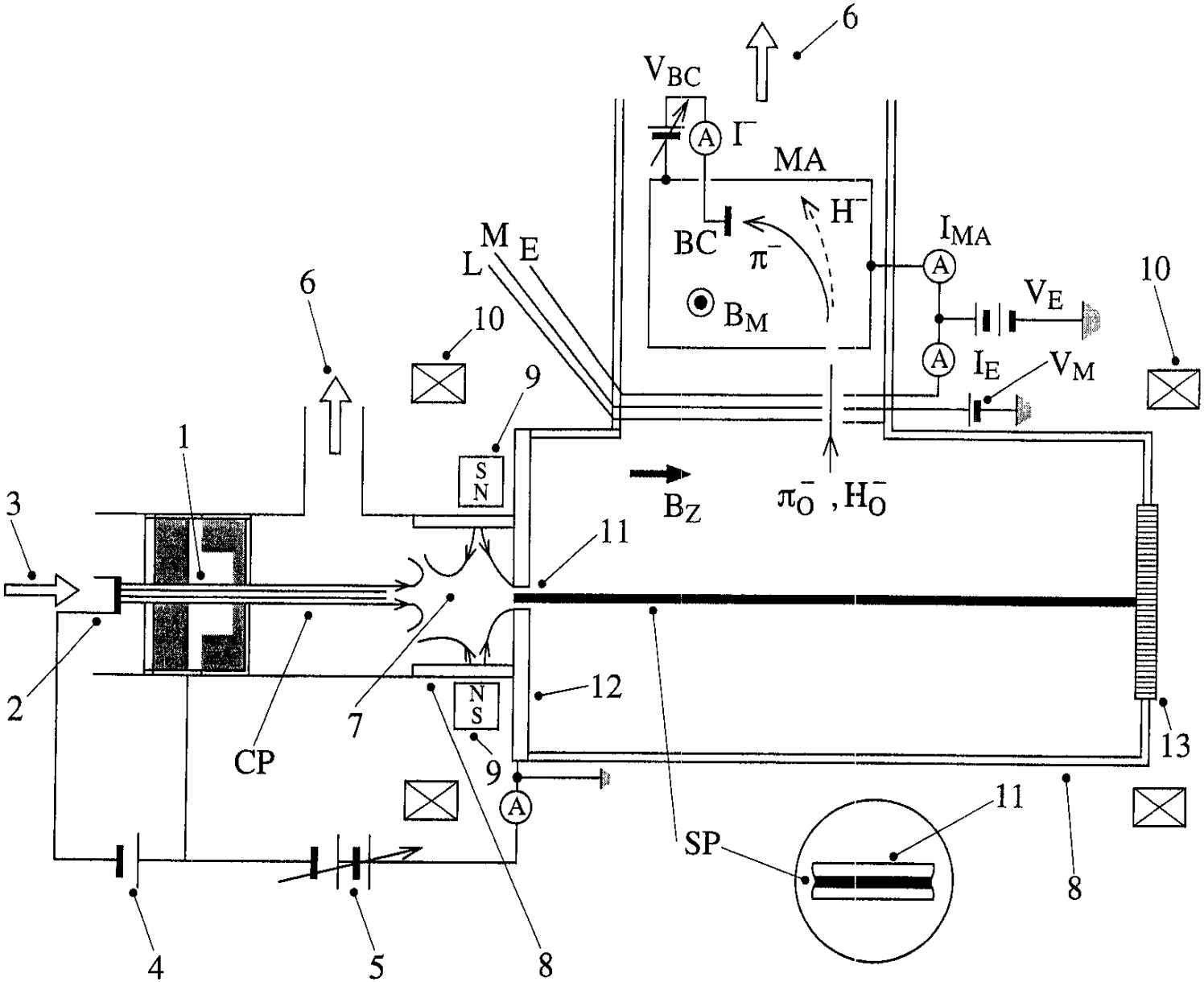
6
V_{BC}
A
I^-
MA
H^-
BC
π^-
B_M
M
L
E
I_{MA}
A
V_E
10
A
I_E
V_M
10
6
10
9
1
S
N
B_Z
π_O^- , H_O^-
3
11
2
CP
7
N
S
12
13
9
A
11
SP
8
4
5
8

Fig. 1

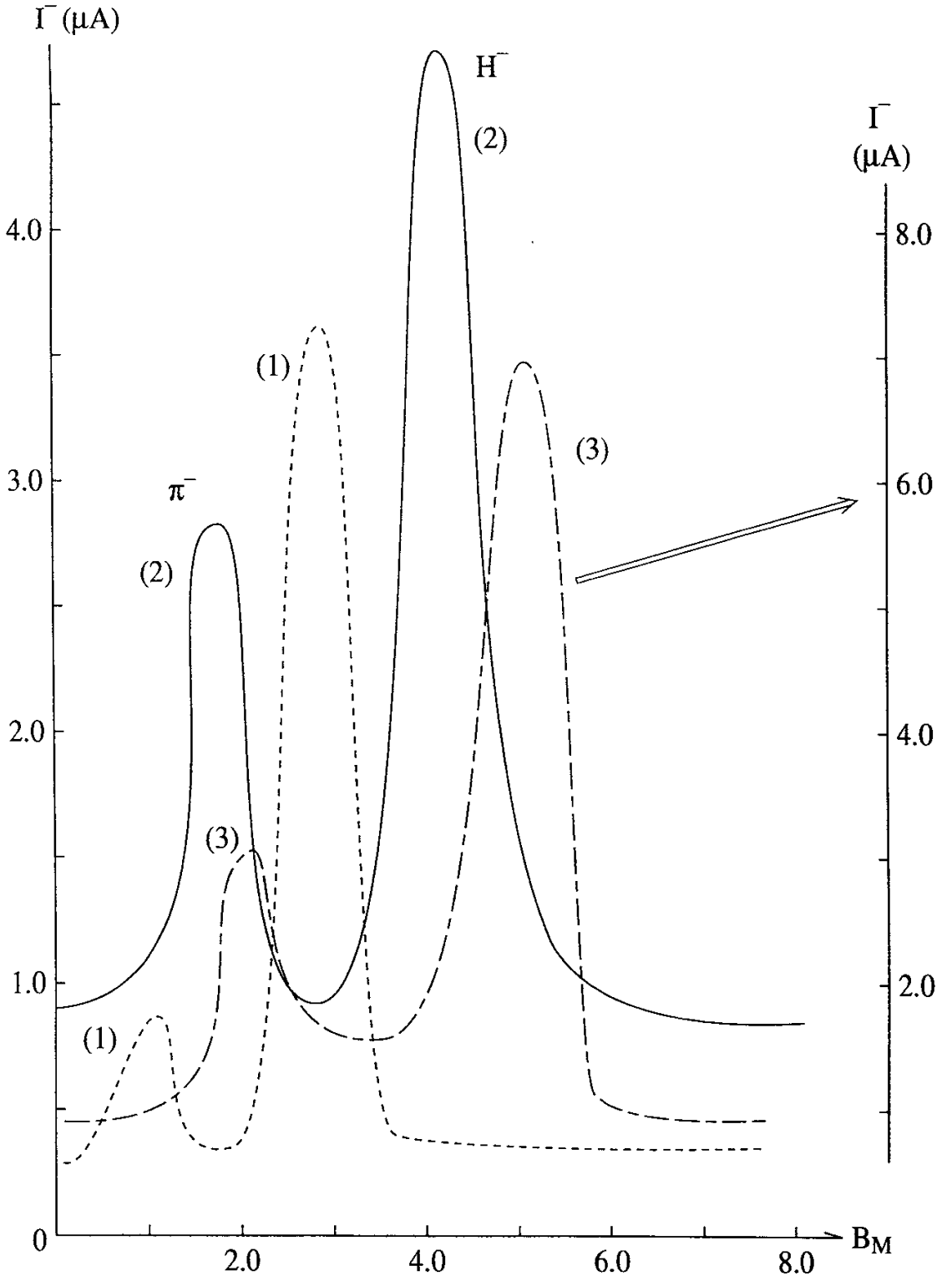

Fig. 2

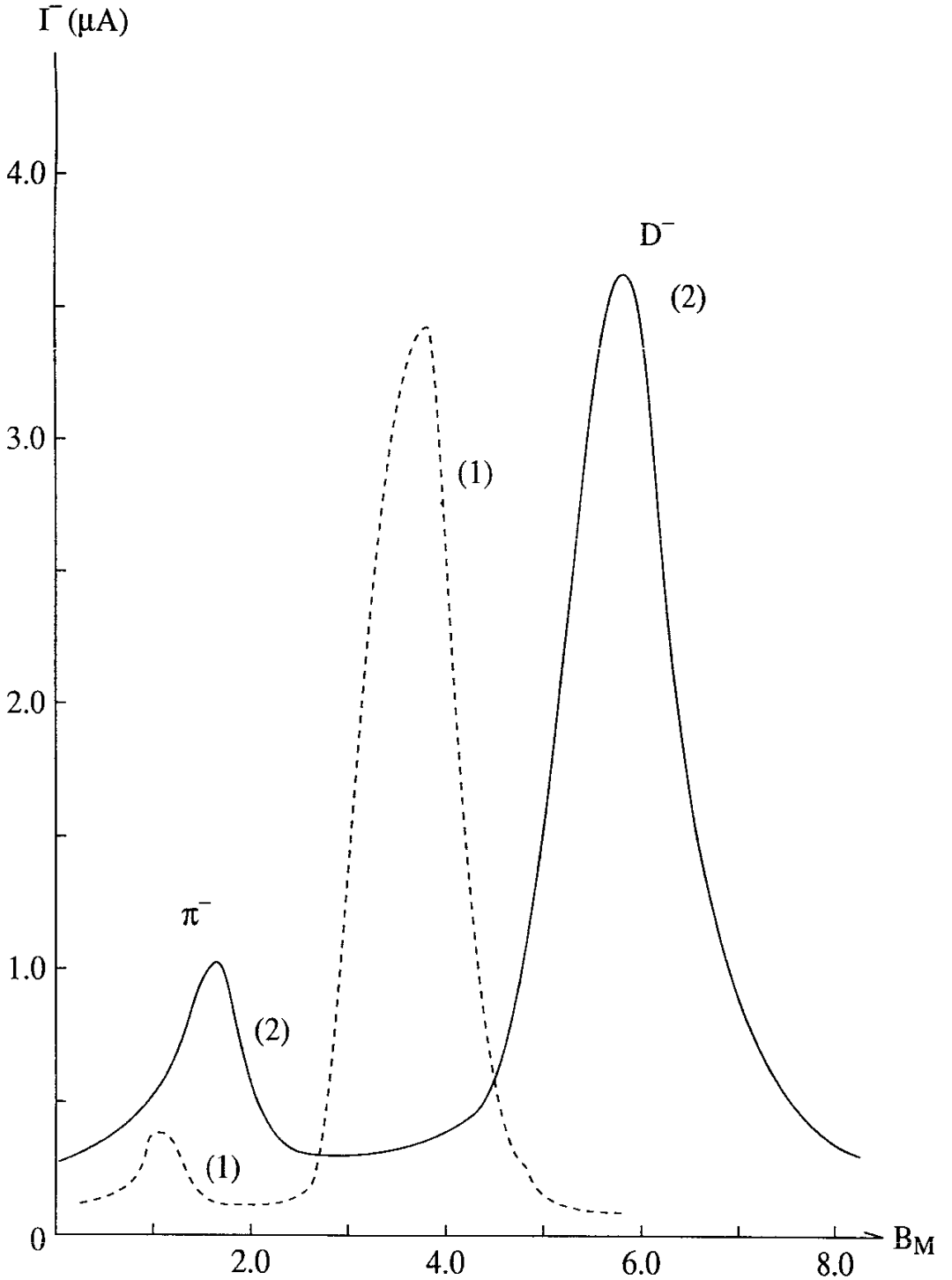

Fig. 3

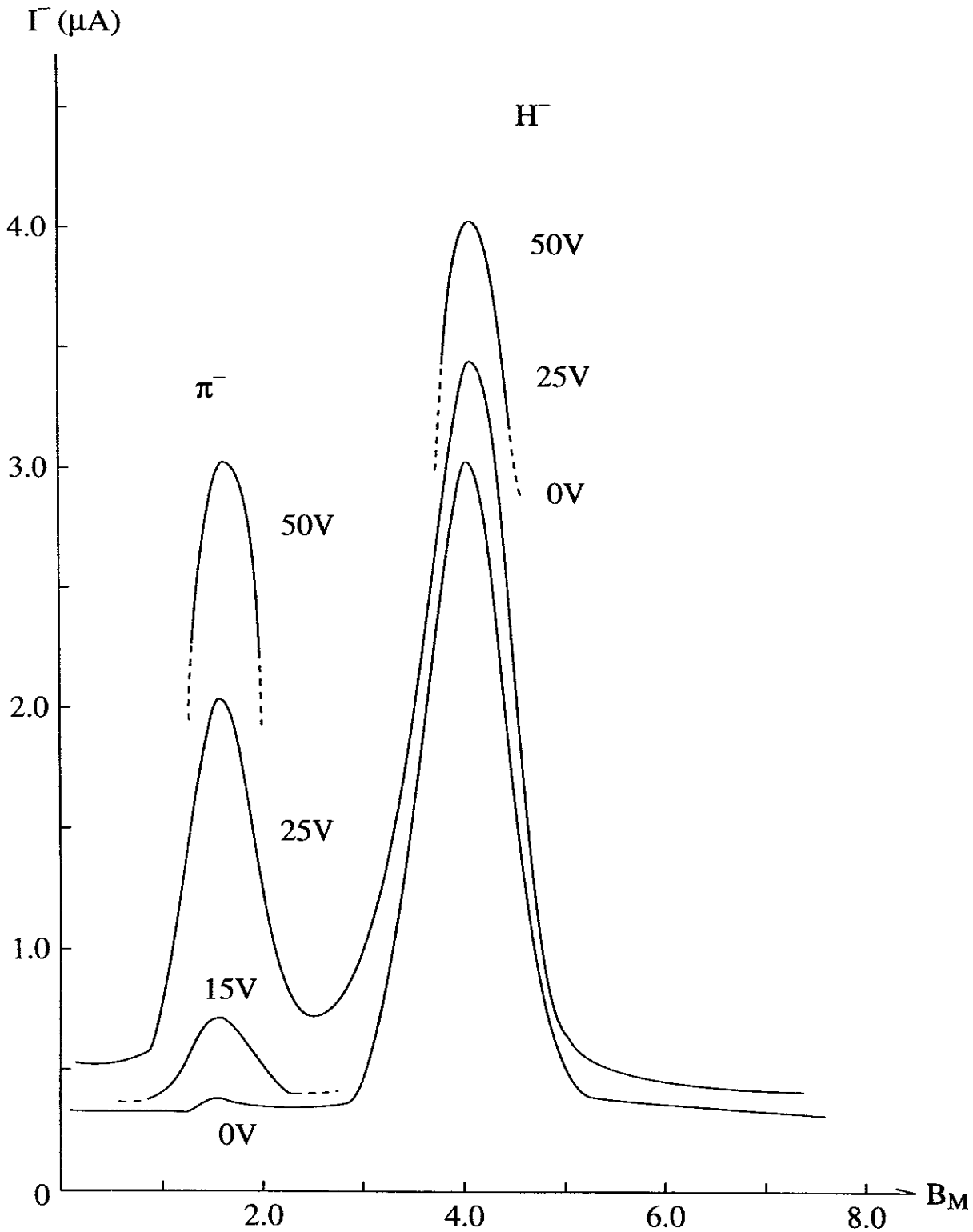
I⁻ (μA)
H⁻
4.0
50V
π⁻
25V
3.0
0V
50V
2.0
25V
1.0
15V
0V
0
2.0
4.0
6.0
8.0
B_M
(×240 Gauss)

Fig. 4

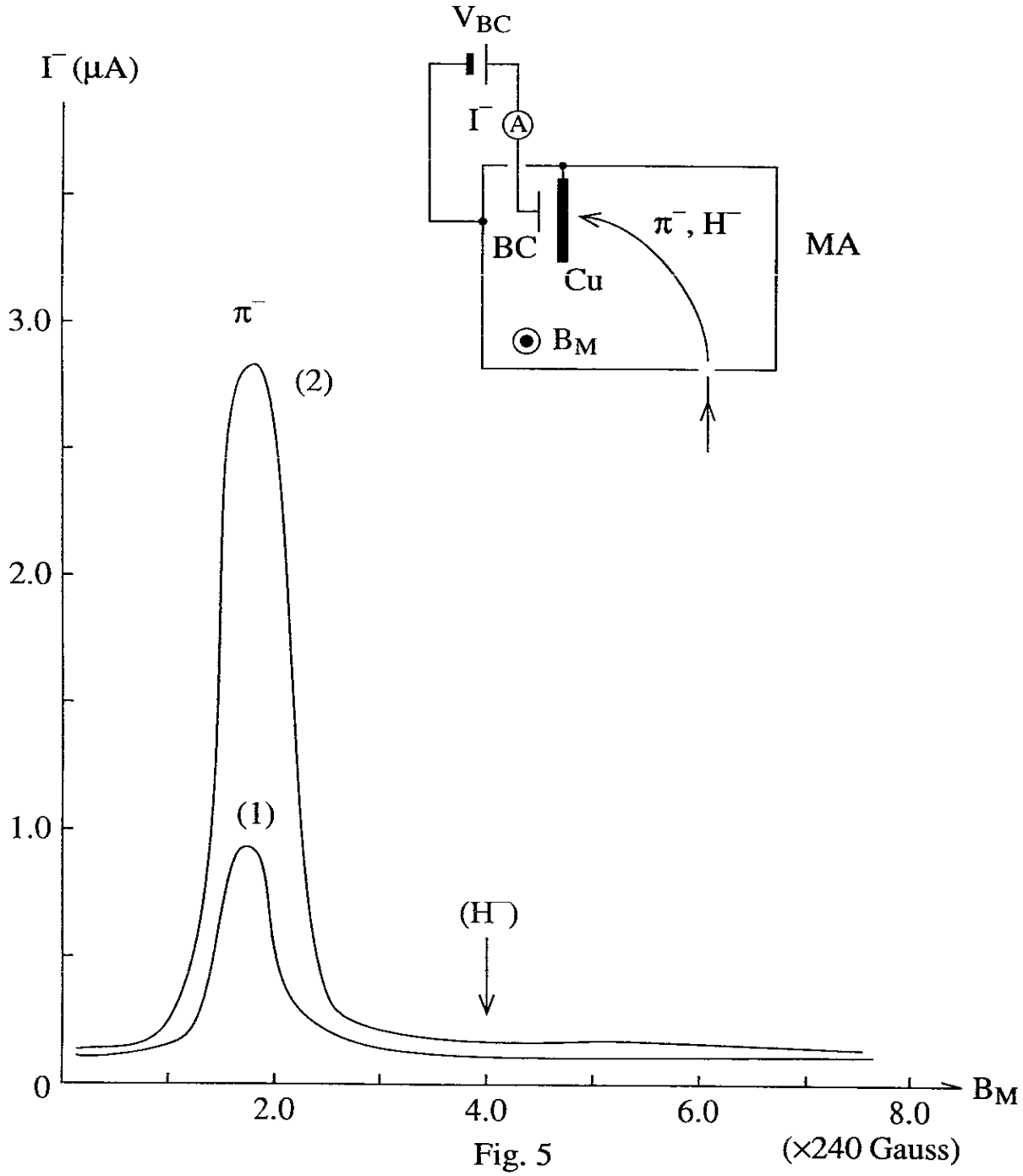

Fig. 5

Appendix

In the above experiments, a question remains: The first peak of I^- may be caused by any unknown mechanism inside the mass analyzer. To dissolve this question, an additional magnetic field of about 150 gauss by a permanent magnet PM is applied near the extraction electrodes as shown in Fig. A1. Thus, some negatively charged particles are extracted from the sheet plasma by the D_2 gas discharge at an extraction voltage $V_E = 800V$. Then, as shown in Fig. A1, the first peak of I^- corresponding to the pionlike particles, disappears while only the second peak of I^- corresponding to D^- ions appears. This reason is due to reduction of cyclotron radius of the pionlike particle π^-. That is, the cyclotron radius becomes below 8 cm while the extracted beam orbit of π^- is curved before entering inside of the mass analyzer. By this experiment of Fig. A1, it is proved that the pionlike particles are extracted from the sheet plasma.

Dependences of the negative current I^- on the analyzing magnetic field B_M, are shown for $V_E = 200V$ and 400V in Fig. A2, while the first peak of I^- disappears for $V_E = 200V$. We consider a reason that the life time of the pionlike particle π^- becomes very short. If the like time of π^- is equal to that of the true pion $\tau \approx 2.6 \times 10^{-8}$ sec, the initial first peak current is reduced by a factor α of exp $(-7.4 \times 10/\sqrt{V_E})$ which is estimated from the total flight distance of 9.8 cm. For $V_E = 200V$, we can estimate $\alpha \approx 5.3 \times 10^{-3}$. That is, for $V_E \leq 200V$, the initial first peak current decays abruptly.[A1)]

Dependences of the negative current I^- on B_M are shown in Fig. A3 for the first extraction electrode voltages V_L ranging from –30V to +10V. At the floating potential $V_L \approx -15V$, both the first and second peak current show a maximum. That is, the first peak current corresponding to the pionlike particles becomes maximum when the H^- ions are produced most efficiently as reported already.[A2, A3)]

Finally, dependences of the negative current I^- on B_M for each case of He or Ar gas discharge, are shown under $V_E = 800V$ in Fig. A4. Both the first peak and the second peak of I^- do not appear except the very small peak due to a small amount of H_2 gas mixed in the He or Ar gas.

Figure Captions of Appendix

Fig. A1 Dependences of negative current I^- on analyzing magnetic field B_M at an extraction voltage V_E = 800V under an additional permanent magnetic PM. (See Fig. 1 also). (1): A case without PM. (2): A case with PM. π^-: Peak of pionlike particles. D^-: Peak of D^- ions. V_{BC} = 100V.

Fig. A2 Dependences of negative current I^- on B_M for extraction voltages of (1) V_E = 200V and (2) V_E = 400V.

Fig. A3 Dependences of I^- on B_M for the first exaction electrode voltages V_L. (A): V_L = −15V (floating). (B): V_L = −30V. (C): V_L = +10V.

Fig. A4 Dependences of I^- on B_M at V_E = 800V under He or Ar gas discharge. He gas pressure: 1.8×10^{-3} Torr. Ar gas pressure: 4.5×10^{-4} Torr.

References of Appendix

A1) J. Uramoto: National Institute of Fusion Science, Nagoya, Japan-Research Report, NIFS-351 (1995).

A2) J. Uramoto: Journal of the vacuum society of Japan, 27 (1984) 600 in Japanese.

A3) J. Uramoto: Journal of the vacuum society of Japan, 27 (1984) 610 in Japanese.

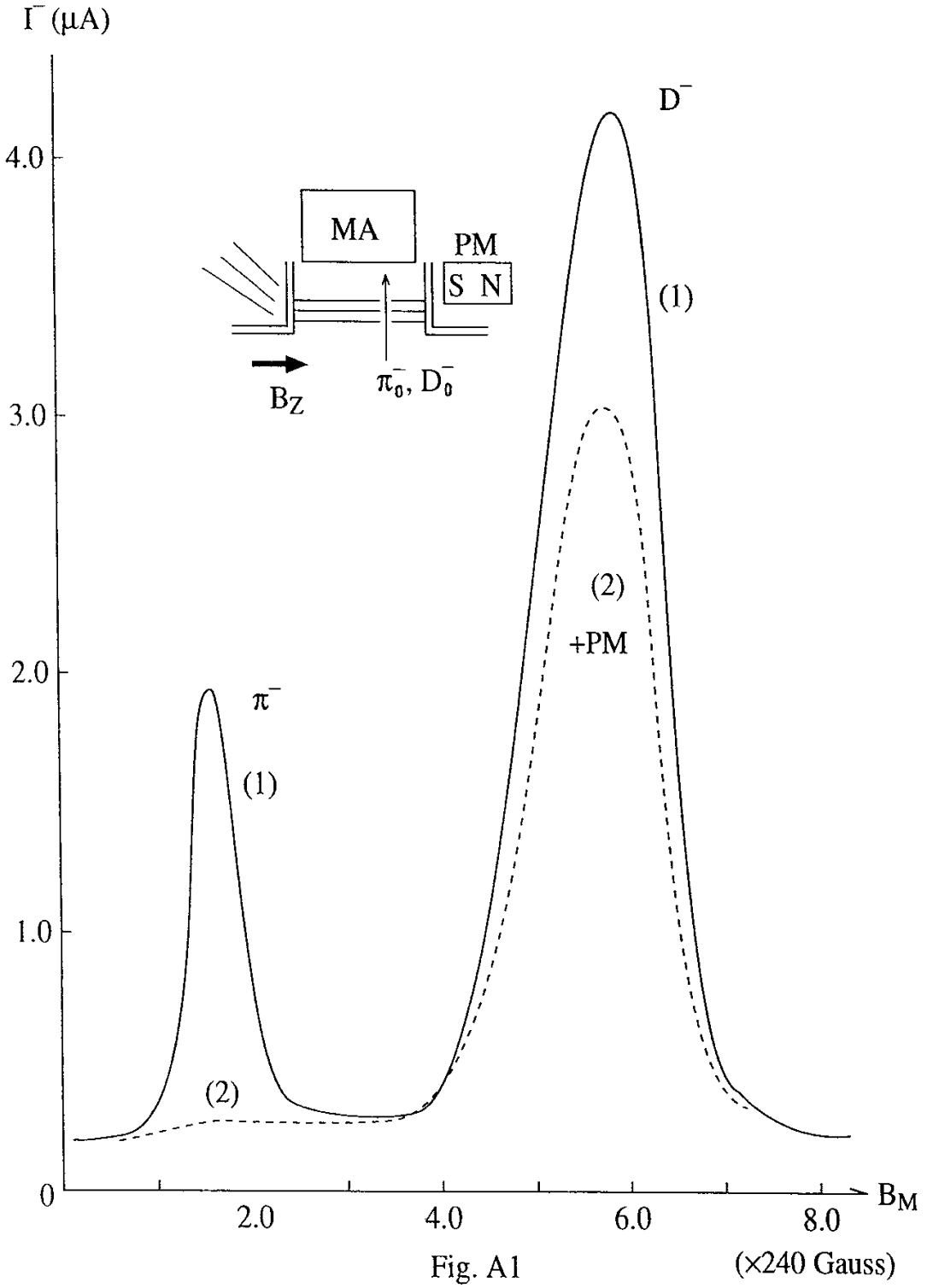
I⁻ (μA)
4.0
3.0
2.0
1.0
0
MA
PM
S N
B_Z
π_0^-, D_0^-
D^-
(1)
(2)
+PM
π^-
(1)
(2)
2.0
4.0
6.0
8.0
B_M
(×240 Gauss)

Fig. A1

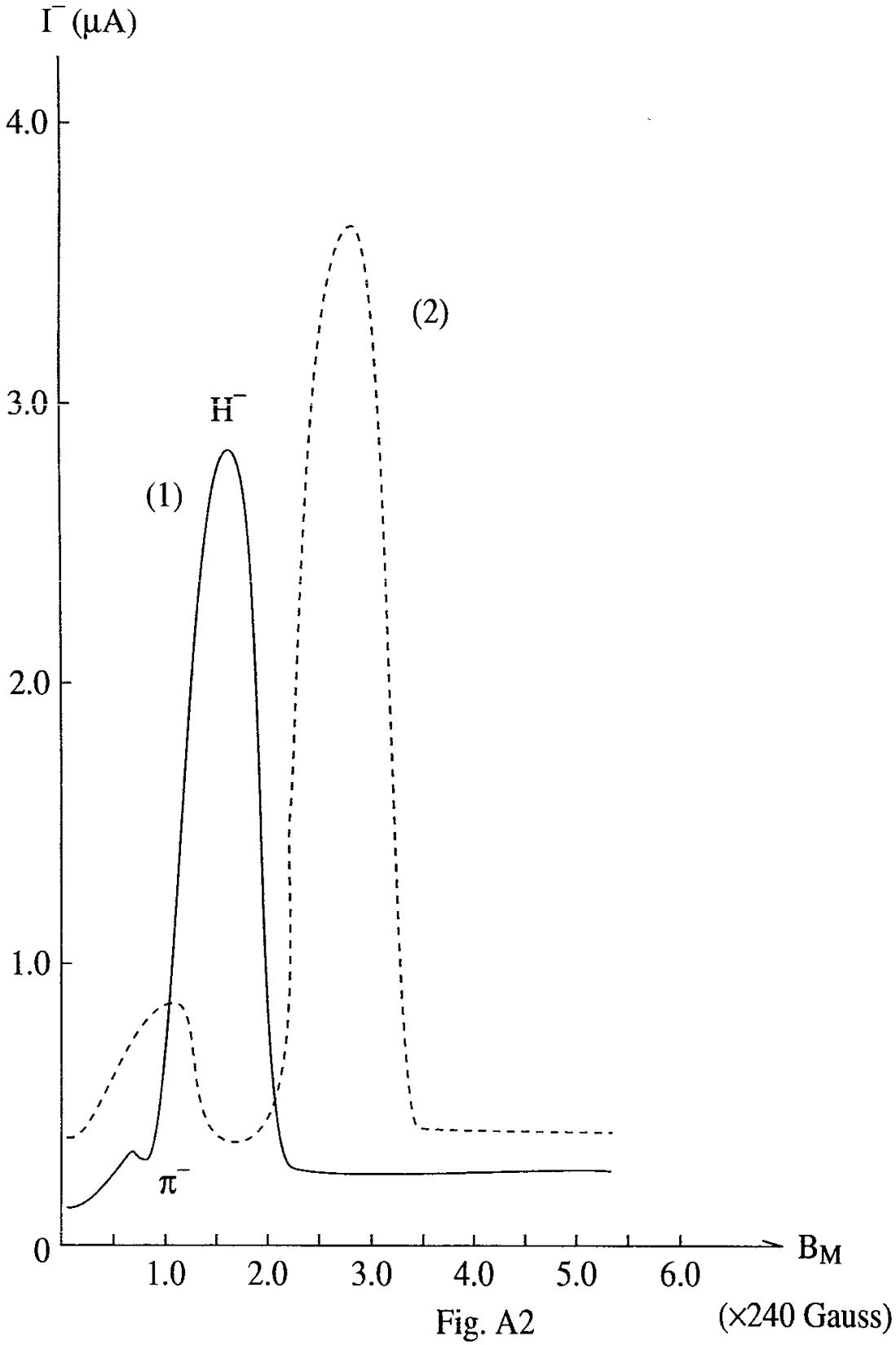

Fig. A2

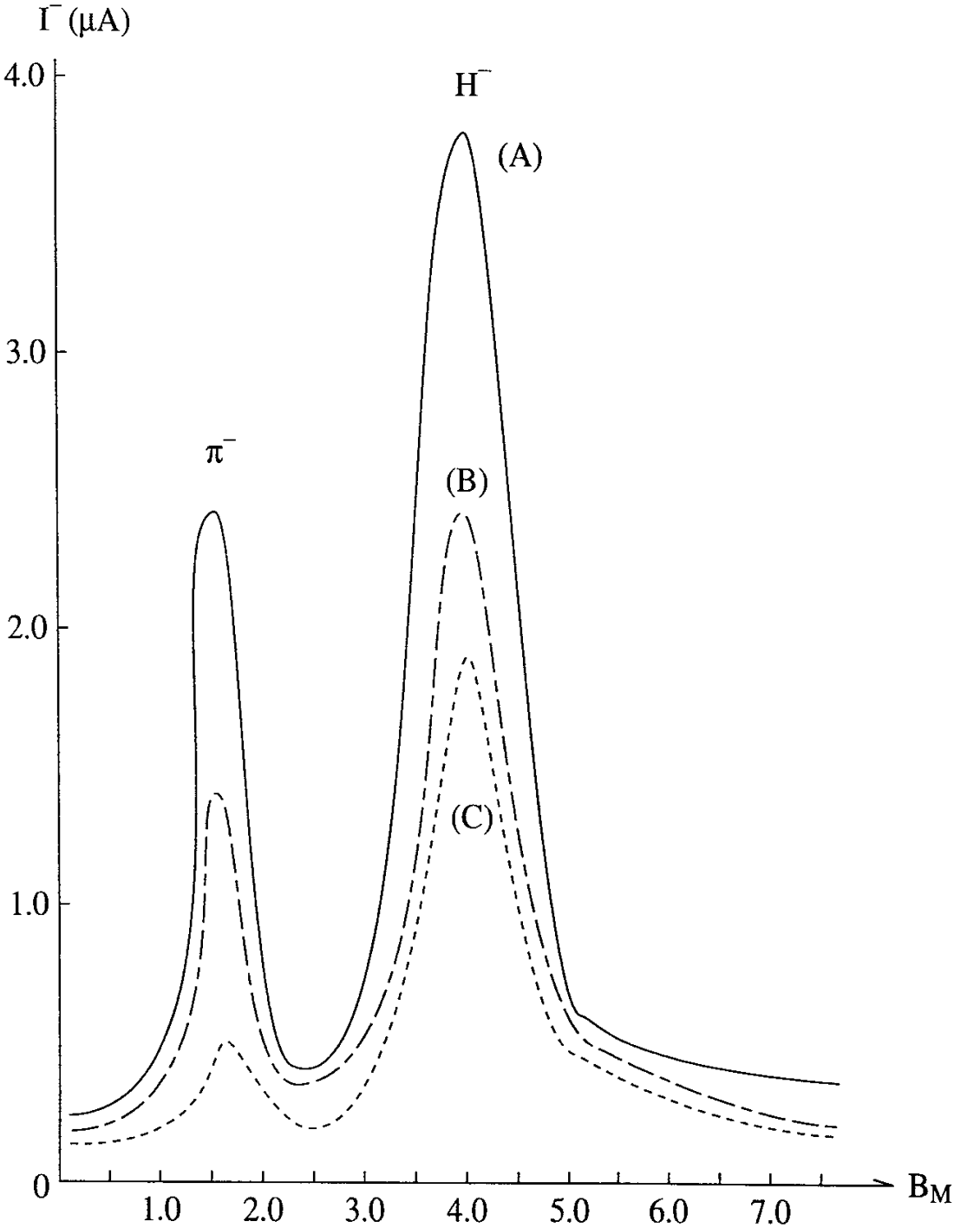

Fig. A3

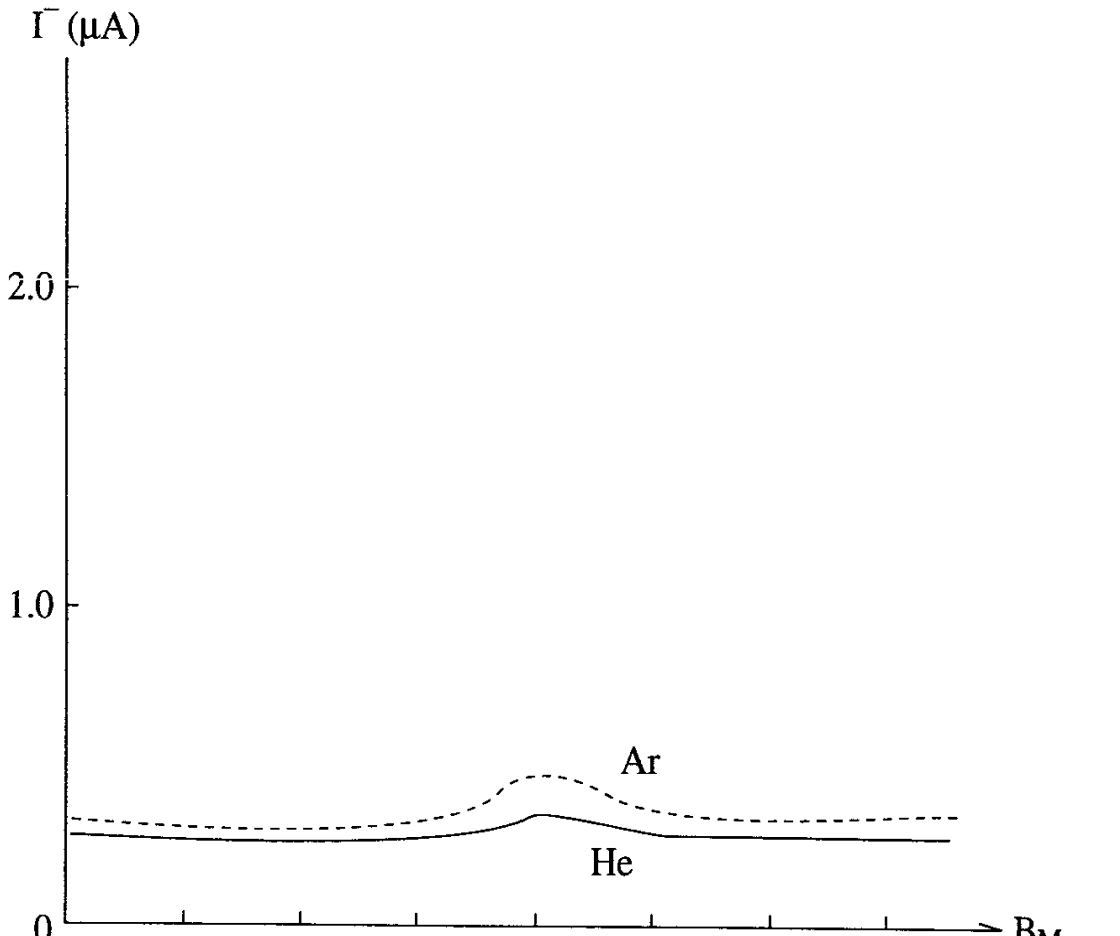

Fig. A4

Recent Issues of NIFS Series

NIFS-329 K. Itoh, S-I. Itoh and A. Fukuyama,
A Model of Sawtooth Based on the Transport Catastrophe; Dec. 1994

NIFS-330 K. Nagasaki, A. Ejiri,
Launching Conditions for Electron Cyclotron Heating in a Sheared Magnetic Field; Jan. 1995

NIFS-331 T.H. Watanabe, Y. Todo, R. Horiuchi, K. Watanabe, T. Sato,
An Advanced Electrostatic Particle Simulation Algorithm for Implicit Time Integration; Jan. 1995

NIFS-332 N. Bekki and T. Karakisawa,
Bifurcations from Periodic Solution in a Simplified Model of Two-dimensional Magnetoconvection; Jan. 1995

NIFS-333 K. Itoh, S.-I. Itoh, M. Yagi, A. Fukuyama,
Theory of Anomalous Transport in Reverse Field Pinch; Jan. 1995

NIFS-334 K. Nagasaki, A. Isayama and A. Ejiri
Application of Grating Polarizer to 106.4GHz ECH System on Heliotron-E; Jan. 1995

NIFS-335 H. Takamaru, T. Sato, R. Horiuchi, K. Watanabe and Complexity Simulation Group,
A Self-Consistent Open Boundary Model for Particle Simulation in Plasmas; Feb. 1995

NIFS-336 B.B. Kadomtsev,
Quantum Telegragh : is it possible?; Feb. 1995

NIFS-337 B.B.Kadomtsev,
Ball Lightning as Self-Organization Phenomenon; Feb. 1995

NIFS-338 Y. Takeiri, A. Ando, O. Kaneko, Y. Oka, K. Tsumori, R. Akiyama, E. Asano, T. Kawamoto, M. Tanaka and T. Kuroda,
High-Energy Acceleration of an Intense Negative Ion Beam; Feb. 1995

NIFS-339 K. Toi, T. Morisaki, S. Sakakibara, S. Ohdachi, T.Minami, S. Morita, H. Yamada, K. Tanaka, K. Ida, S. Okamura, A. Ejiri, H. Iguchi, K. Nishimura, K. Matsuoka, A. Ando, J. Xu, I. Yamada, K. Narihara, R. Akiyama, H. Idei, S. Kubo, T. Ozaki, C. Takahashi, K. Tsumori,
H-Mode Study in CHS; Feb. 1995

NIFS-340 T. Okada and H. Tazawa,
Filamentation Instability in a Light Ion Beam-plasma System with External Magnetic Field; Feb. 1995

NIFS-341 T. Watanbe, G. Gnudi,
A New Algorithm for Differential-Algebraic Equations Based on HIDM;
Feb. 13, 1995

NIFS-342 Y. Nejoh,
New Stationary Solutions of the Nonlinear Drift Wave Equation;
Feb. 1995

NIFS-343 A. Ejiri, S. Sakakibara and K. Kawahata,
Signal Based Mixing Analysis for the Magnetohydrodynamic Mode Reconstruction from Homodyne Microwave Reflectometry; Mar.. 1995

NIFS-344 B.B.Kadomtsev, K. Itoh, S.-I. Itoh
Fast Change in Core Transport after L-H Transition; Mar. 1995

NIFS-345 W.X. Wang, M. Okamoto, N. Nakajima and S. Murakami,
An Accurate Nonlinear Monte Carlo Collision Operator; Mar. 1995

NIFS-346 S. Sasaki, S. Takamura, S. Masuzaki, S. Watanabe, T. Kato, K. Kadota,
Helium I Line Intensity Ratios in a Plasma for the Diagnostics of Fusion Edge Plasmas; Mar. 1995

NIFS-347 M. Osakabe,
Measurement of Neutron Energy on D-T Fusion Plasma Experiments;
Apr. 1995

NIFS-348 M. Sita Janaki, M.R. Gupta and Brahmananda Dasgupta,
Adiabatic Electron Acceleration in a Cnoidal Wave; Apr. 1995

NIFS-349 J. Xu, K. Ida and J. Fujita,
A Note for Pitch Angle Measurement of Magnetic Field in a Toroidal Plasma Using Motional Stark Effect; Apr. 1995

NIFS-350 J. Uramoto,
Characteristics for Metal Plate Penetration of a Low Energy Negative Muonlike or Pionlike Particle Beam: Apr. 1995

NIFS-351 J. Uramoto,
An Estimation of Life Time for A Low Energy Negative Pionlike Particle Beam: Apr. 1995

NIFS-352 A. Taniike,
Energy Loss Mechanism of a Gold Ion Beam on a Tandem Acceleration System: May 1995

NIFS-353 A. Nishizawa, Y. Hamada, Y. Kawasumi and H. Iguchi,
Increase of Lifetime of Thallium Zeolite Ion Source for Single-Ended Accelerator: May 1995

NIFS-354 S. Murakami, N. Nakajima, S. Okamura and M. Okamoto,
Orbital Aspects of Reachable β Value in NBI Heated Heliotron/Torsatrons; May 1995

NIFS-355 H. Sugama and W. Horton,
Neoclassical and Anomalous Transport in Axisymmetric Toroidal Plasmas with Electrostatic Turbulence; May 1995

NIFS-356 N. Ohyabu
A New Boundary Control Scheme for Simultaneous Achievement of H-mode and Radiative Cooling (SHC Boundary); May 1995

NIFS-357 Y. Hamada, K.N. Sato, H. Sakakita, A. Nishizawa, Y. Kawasumi, R. Liang, K. Kawahata, A. Ejiri, K. Toi, K. Narihara, K. Sato, T. Seki, H. Iguchi, A. Fujisawa, K. Adachi, S. Hidekuma, S. Hirokura, K. Ida, M. Kojima, J. Koong, R. Kumazawa, H. Kuramoto, T. Minami,. M. Sasao, T. Tsuzuki, J.Xu, I. Yamada, and T. Watari,
Large Potential Change Induced by Pellet Injection in JIPP T-IIU Tokamak Plasmas; May 1995

NIFS-358 M. Ida and T. Yabe,
Implicit CIP (Cubic-Interpolated Propagation) Method in One Dimension; May 1995

NIFS-359 A. Kageyama, T. Sato and The Complexity Simulation Group,
Computer Has Solved A Historical Puzzle: Generation of Earth's Dipole Field; June 1995

NIFS-360 K. Itoh, S.-I. Itoh, M. Yagi and A. Fukuyama,
Dynamic Structure in Self-Sustained Turbulence; June 1995

NIFS-361 K. Kamada, H. Kinoshita and H. Takahashi,
Anomalous Heat Evolution of Deuteron Implanted Al on Electron Bombardment; June 1995

NIFS-362 V.D. Pustovitov,
Suppression of Pfirsch-schlüter Current by Vertical Magnetic Field in Stellarators; June 1995

NIFS-363 A. Ida, H. Sanuki and J. Todoroki
An Extended K-dV Equation for Nonlinear Magnetosonic Wave in a Multi-Ion Plasma; June 1995

NIFS-364 H. Sugama and W. Horton
Entropy Production and Onsager Symmetry in Neoclassical Transport Processes of Toroidal Plasmas; July 1995

NIFS-365 K. Itoh, S.-I. Itoh, A. Fukuyama and M. Yagi,

On the Minimum Circulating Power of Steady State Tokamaks; July 1995

NIFS-366 K. Itoh and Sanae-I. Itoh,
The Role of Electric Field in Confinement; July 1995

NIFS-367 F. Xiao and T. Yabe,
A Rational Function Based Scheme for Solving Advection Equation; July 1995

NIFS-368 Y. Takeiri, O. Kaneko, Y. Oka, K. Tsumori, E. Asano, R. Akiyama, T. Kawamoto and T. Kuroda,
Multi-Beamlet Focusing of Intense Negative Ion Beams by Aperture Displacement Technique; Aug. 1995

NIFS-369 A. Ando, Y. Takeiri, O. Kaneko, Y. Oka, K. Tsumori, E. Asano, T. Kawamoto, R. Akiyama and T. Kuroda,
Experiments of an Intense H- Ion Beam Acceleration; Aug. 1995

NIFS-370 M. Sasao, A. Taniike, I. Nomura, M. Wada, H. Yamaoka and M. Sato,
Development of Diagnostic Beams for Alpha Particle Measurement on ITER; Aug. 1995

NIFS-371 S. Yamaguchi, J. Yamamoto and O. Motojima;
A New Cable -in conduit Conductor Magnet with Insulated Strands; Sep. 1995

NIFS-372 H. Miura,
Enstrophy Generation in a Shock-Dominated Turbulence; Sep. 1995

NIFS-373 M. Natsir, A. Sagara, K. Tsuzuki, B. Tsuchiya, Y. Hasegawa, O. Motojima,
Control of Discharge Conditions to Reduce Hydrogen Content in Low Z Films Produced with DC Glow; Sep. 1995

NIFS-374 K. Tsuzuki, M. Natsir, N. Inoue, A. Sagara, N. Noda, O. Motojima, T. Mochizuki, I. Fujita, T. Hino and T. Yamashina,
Behavior of Hydrogen Atoms in Boron Films during H_2 and He Glow Discharge and Thermal Desorption; Sep. 1995

NIFS-375 U. Stroth, M. Murakami, R.A. Dory, H. Yamada, S. Okamura, F. Sano and T. Obiki,
Energy Confinement Scaling from the International Stellarator Database; Sep. 1995

NIFS-376 S. Bazdenkov, T. Sato, K. Watanabe and The Complexity Simulation Group,
Multi-Scale Semi-Ideal Magnetohydrodynamics of a Tokamak Plasma; Sep. 1995